ELSEVIER

Journal of Alloys and Compounds 271–273 (1998) 522–529

Journal of ALLOYS AND COMPOUNDS

Actinide transmutation properties of thermal and fast fission reactors including multiple recycling

H.W. Wiese*

Forschungszentrum Karlsruhe, Institut für Neutronenphysik und Reaktortechnik, Postfach 3640, 76021 Karlsruhe, Germany

Abstract

To decrease the long-term radiotoxicity risk from nuclear waste, investigations were performed to transmute long-lived radwaste nuclides: actinides, in particular isotopes of Pu, Np, Am, and fission products, to short-lived or stable nuclei. First, from neutron spectra and resulting neutron reaction cross-sections, transmutation half-lives, and fission-to-capture ratios, the priority of fast over thermal reactors with respect to transmutation is derived. Second, transmutation calculations for a park of PWRs and fast CAPRA burner reactors show the ability of CAPRAs to reduce Pu and minor actinides with homogeneous multiple recycling of Pu and Np and heterogeneous multiple recycling of Am. Accumulation of 1st generation PWR-Pu is stopped. Because of Pu deterioration, reactivity requirements and Pu≤45 % in (U,Pu)-MOX, 58 % of 'bad quality' and proliferation-resistant Pu from reprocessing of spent CAPRA fuel has to be excluded from recycling. Homogeneous 5 % admixing of Np results in a constant-level Np park inventory. The relatively large consumption of Am is counteracted by a significant in-core production of Am, resulting in a net increase of park Am. © 1998 Elsevier Science S.A.

Keywords: Reactors; Actinides; Transmutation; Recycling

1. Introduction

Production of electric energy by nuclear reactors entails production of plutonium and radioactive waste. To minimize the long-term radiotoxicity risk for future generations of man, a moral demand to present consumers, theoretical and experimental investigations mainly in Europe and Japan are underway to transmute long-lived radioactive waste nuclides: actinides, in particular Pu, minor actinides (MA) Np, Am, and selected fission products, to short-lived or stable species. Special attention is paid to utilization and incineration of Pu accumulating from thermal-reactor operation.

2. Neutron spectra and transmutation cross-sections

Fission neutrons are generated with an average energy of about 2 MeV, some reaching up to 10 MeV. They are scattered by heavy nuclei, losing a relative amount of energy $\Delta E/E \geq 1/A$, A=mass number of the scattering nucleus, and by light nuclei, being thermalized after 18 collisions in the case of hydrogen. Scattering does not directly result in a transmutation, i.e. a change of the charge number Z or the number of neutrons N of the original nucleus $[Z,N]$, but it alters the energy distribution of neutrons, the neutron spectrum.

Most transmutations in fission reactors are initiated by neutron absorptions, causing either fission and hence generation of fission products, or emission of γ-rays, leaving a nucleus of the same element but with one additional neutron: $[Z, N]$ (n, γ) $[Z, N+1]$. Furthermore, there are transmutations by (n, 2n)-reactions, resulting in a nucleus of the same element but with one less neutron, $[Z, N]$ (n, 2n) $[Z, N\text{-}1]$. Additional Z or N changing interactions are radioactive decays: β^-, β^+, and α-decays, leading to $[Z+1, N]$, $[Z\text{-}1, N]$, and $[Z\text{-}2, N\text{-}2]$, respectively.

In a critical reactor at time t after start-up, the field of neutrons is described by the vector flux density $\Phi(r, \Omega, E, t)$ with r=location, Ω=direction of flight, and E=neutron energy, as a solution of the homogeneous Boltzmann neutron transport equation with power normalization. Integration of $\Phi(r, \Omega, E, t)$ by directions gives the scalar flux density $\Phi(r, E, t)$ which, integrated by energy, results in the space and time dependent total neutron flux $\Phi(r, t)$. The neutron spectrum is defined by $\chi(r, E, t) = \Phi(r, E, t)/\Phi(r, t)$ with $\chi(r, E, t)\,dE$ giving the fraction of neutrons

*Fax: +49 7247 824874; e-mail: wiese@inr.fzk.de

0925-8388/98/$19.00
PII: S0925-8388(98)00141-8

with energies between E and $E+\mathrm{d}E$ at location r and time t.

To find out the parameters responsible for creation and transmutation of nuclei, Pu241 as a typical example is considered, concentrating on the reactions Pu241 (β^-) Am241, Pu241 (n, γ) Pu242, Pu241 (n, f) fission products, Pu240 (n, γ) Pu241. The total rate of change of the number N of Pu241 nuclei per cm^3 at r and t is

$$\frac{\mathrm{d}}{\mathrm{d}t}N_{\mathrm{Pu241}}(t) = -\lambda N_{\mathrm{Pu241}}(t) \quad \text{(decay)}$$

$$-(\sigma_{\mathrm{c,Pu241}} + \sigma_{\mathrm{f,Pu241}})\Phi\, N_{\mathrm{Pu241}}(t) \quad \text{(transmutation)} \qquad (1)$$

$$+\sigma_{\mathrm{c,Pu240}}\Phi\, N_{\mathrm{Pu240}}(t) \quad \text{(creation)}$$

For simplicity, the space variable r is omitted. As usual, λ and $\sigma_{\mathrm{x,n}}$ are the decay constant and the microscopic cross-sections for reaction x at nuclide n, respectively. In Eq. (1), $\lambda N(t)$ is the decay rate, Φ the total flux, and $\sigma\Phi N(t)$ are neutron reaction rates at time t. The effective reaction cross-sections $\sigma_{\mathrm{x,n}}$ are given by

$$\sigma_{\mathrm{x,n}}(r,t) = \int_{0.001\ \mathrm{eV}}^{10\ \mathrm{MeV}} \mathrm{d}E\ \sigma_{\mathrm{x,n}}(E)\chi(r,E,t)$$
$$= \int_0^{23.03} \mathrm{d}u\ \sigma_{\mathrm{x,n}}(u)[E\chi(r,E,t)](u) \qquad (2)$$

where the lethargy $u=\ln(E_0/E)$, $E_0=10$ MeV, is chosen as the integration variable. The dimensionless lethargy distribution $\phi(u)=[E\chi(r,\ E,\ t)]\ (u)$ is often referred to as 'neutron spectrum'.

The effective reaction cross-section is a function of the reaction cross-section $\sigma_{\mathrm{x,n}}(E)$ evaluated from measurements and compiled in Nuclear Data Files as the Joint Evaluated File, JEF [1], and of the reactor, space and time dependent neutron spectrum $\chi(r,\ E,\ t)$. Furthermore, the rate of change depends on the total neutron flux $\Phi(r,\ t)$, i.e. on the local power at time t, and on the number densities of reacting nuclides. Corresponding to the fact that in numerical calculations the coupled system of differential equations of type (1), the so-called 'System of Burn-Up and Decay Equations', may be solved with stepwise constant-in-time coefficients, in Eq. (1) the time dependence of the effective cross-sections is not explicitly denoted.

In Fig. 1 the typical neutron spectra $\phi(u)$ in thermal and fast reactors is presented. Spectra in light-water moderated PWRs characteristically show the peak of fission neutrons around 2 MeV, the slowing-down region with $\Phi(E)\sim 1/E$ down to about 1 eV, and the thermal region with neutrons in scattering equilibrium with hydrogen atoms in water. These spectra from the Boltzmann equation in a multi-energy-group approximation [2], however, do not represent the spectrum fine-structure for energies from about 10 eV to 20 keV; the resonance region of heavy materials. These small-width but numerous resonances affect the neutron

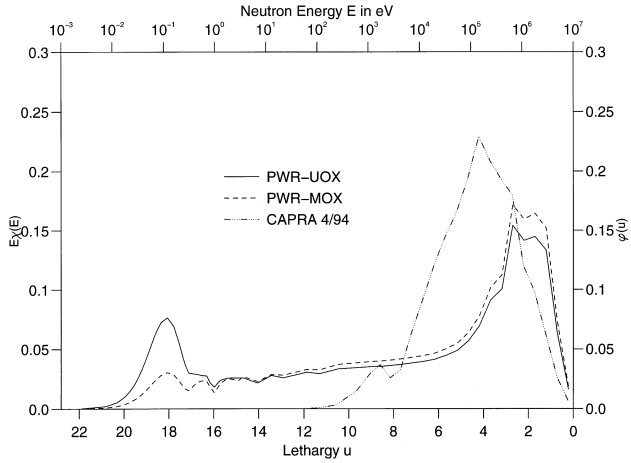

Fig. 1. Mean burn-up neutron neutron spectra in fission reactors.

flux density principally in the same way as wide resonances do, e.g. the neutron capture resonances of Pu240 at 1 eV or the resonances of Pu239 at 0.3 eV, leading to dips in the spectrum around the resonance energies. In the PWR-MOX spectrum, due to plutonium in MOX fuel, the thermal part is less pronounced compared to the PWR-UOX spectrum. In sodium-cooled fast reactors such as the French plutonium burner reactor of type CAPRA [3], due to the lack of low-mass number scatterers, thermalization of neutrons needs much more collisions, and neutrons are absorbed causing fissions or transmutations before being slowed down. The bulk of neutrons have energies between 100 keV and 1 MeV. At 3 keV, the effect of the sodium scattering resonance is seen.

Spectra in Fig. 1 and cross-sections from Fig. 2 result in differential effective cross-sections shown in Fig. 3. In this representation, the effective spectrum-averaged reaction cross-sections are the areas between the differential cross-section curves and the lethargy axis. Note that in Fig. 2 in the resonance region from 10 eV to about 20 keV including unresolved resonances, only mean values are given.

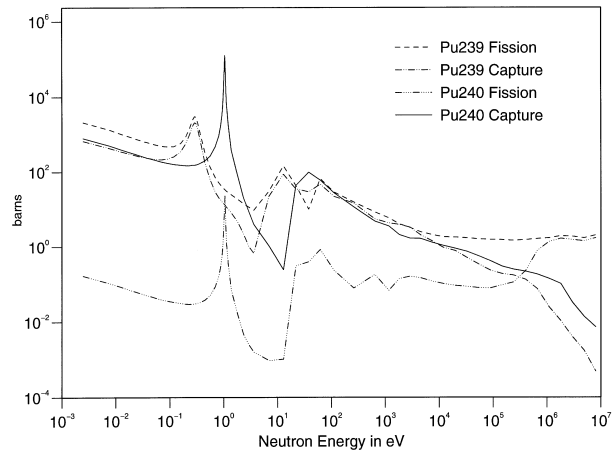

Fig. 2. Neutron reaction cross-sections.

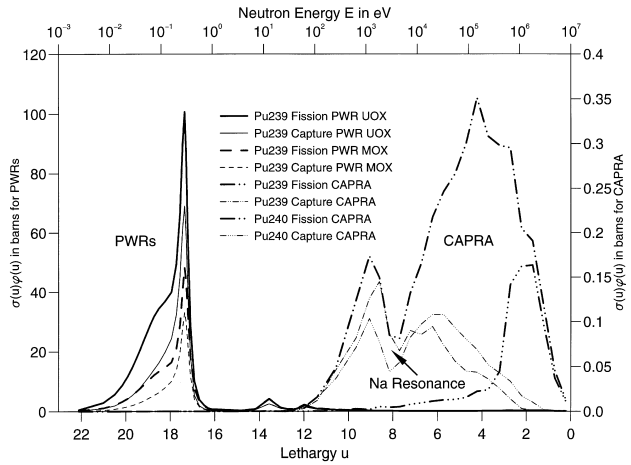

Fig. 3. Pu differential effective cross-sections in PWRs and CAPRA.

Table 1
Effective cross-sections (barns) in thermal and fast reactors

Nuclide	PWR-UOX		PWR-MOX		EFR	
	σ_c	σ_f	σ_c	σ_f	σ_c	σ_f
U 235	9.12	39.2	6.19	21.9	0.564	2.00
U 236	7.07	0.301	8.54	0.339	0.740	0.093
U 238	0.912	0.109	0.866	0.119	0.299	0.044
Np237	33.7	0.516	25.8	0.559	1.58	0.308
Pu238	28.8	2.40	15.1	2.07	0.663	1.03
Pu239	52.5	95.1	25.2	45.8	0.514	1.85
Pu240	133.0	0.625	41.8	0.65	0.405	0.372
Pu241	34.1	101.0	17.4	52.4	0.590	2.63
Pu242	28.6	0.461	19.0	0.492	0.572	0.263
Am241	93.3	1.20	54.8	0.944	1.84	0.279
Am242	307.0	160.0	141.0	86.8	0.653	3.15
Am243	50.0	0.439	41.4	0.468	1.50	0.242
Cm242	4.26	1.13	3.91	1.01	0.560	0.578
Cm244	17.0	1.02	15.0	1.02	0.673	0.431

Since in UOX-PWRs the neutron spectrum during irradiation significantly varies with the build-up of plutonium, in fresh UOX without Pu there are no dips from Pu resonances. For some nuclei effective reaction cross-sections in UOX fuel reveal a significant dependence on fuel irradiation time. In particular, the capture cross-section of Pu240, responsible itself for the flux depression at 1 eV, decreases by about a factor of two with a build-up of plutonium by the effect of resonance self-shielding. The effective $\sigma_{c,Pu240}$ almost exclusively is determined by the height and width of the resonance and the spectrum around 1 eV. Effective capture and fission cross-sections of Pu239 correspond to the areas between the differential cross-sections and the lethargy axis shown in Fig. 3.

For neutron energies above 100 eV relevant in fast reactors, three regions have to be considered: the resonance region up to 20 keV, the region of monotonously decreasing cross-sections up to about 1 MeV, and the region above 1 MeV where threshold reactions as fission of even-numbered U and Pu isotopes enter the scene; see Fig. 2 for Pu240. In Fig. 3 the CAPRA spectrum weighted differential cross-sections of Pu239 and Pu240, being strongly affected by the sodium resonance except for the threshold fission reaction of Pu240 is shown.

Since $\sigma(u)\phi(u)\mathrm{d}uN\Phi$ is the number of reactions in the lethargy interval du at u in a neutron flux density Φ acting on N nuclides per cm^3, representations, as in Fig. 3, are especially suited to show the fission and transmutation properties of nuclei in different reactor neutron spectra.

In Table 1, spectrum-averaged effective cross-sections in PWRs and in the sodium-cooled fast reactor EFR (European Fast Reactor [4]) are listed for a selected number of nuclides. Due to the fact that in general, except for threshold reactions, cross-sections decrease with increasing energy of neutrons, the spectrum-averaged cross-sections decrease from UOX-PWRs via MOX-PWRs to fast reactors. In thermal reactors, predominantly nuclei with odd numbers of neutrons like U233, U235, Pu239, Pu241, Am242 are fissioned. In fast reactors, additionally nuclei with even numbers of neutrons, in particular Pu238, Pu240, Pu242, Am241,..., Cm244 undergo fission by threshold reaction.

An important quantity in transmutation analysis is the spectrum specific fission-to-capture ratio. Both capture and fission lead to a destruction of the concerning nuclide. Capture creates another, in many cases, long-lived actinide, whereas fission on average generates fission products with half-lives of around 30 years. Thus, with respect to a reduction of long-lived waste, predominance of fission is desirable. Fission-to-capture ratios shown in Fig. 4 clearly demonstrate the superiority of fast reactors to thermal reactors.

From Eq. (1) it is seen that the nuclide density rate of change is controlled by $(\sigma_c+\sigma_f)\Phi=\sigma_a\Phi$ having the same dimension 1/s as the decay constant λ. In parallel to the radioactive decay half-life $\tau_{1/2}=0.693/\lambda$, in the context of transmutation, the 'transmutation half-life' $\tau_{trans}=0.693/\sigma_a\Phi$ is frequently used. Short transmutation half-lives obviously are advantageous in actinide burner reactors. In thermal and fast reactors typical neutron flux densities are 1.5×10^{14} n cm^{-2} s^{-1} and 4×10^{15} n cm^{-2} s^{-1}, respectively. Transmutation half-lives in fast reactors for nuclides of interest, see Fig. 4, range between 7 years (Pu240) and 2 years (Pu241). In particular, for the minor actinides Np237, Am241, Am243 in fast reactors, $3<\tau_{trans}<4$ is found. Also with respect to transmutation half-lives, fast reactors turn out to be superior to thermal reactors. Pu240, due to the 1 eV resonance, is contraproductive.

The conclusion from this chapter is: fast reactors, due to their neutron spectrum, are superior to thermal reactors with respect to transmutation of actinides. This conclusion up to now is solely based on the discussion of the transmutation term of the basic Eq. (1) and its generalizations. For the evaluation of creation terms, neutron captures in Pu240 in our specific example, besides $\sigma_{c,Pu240}$, the actual amount of Pu240 has to be known. As a matter of

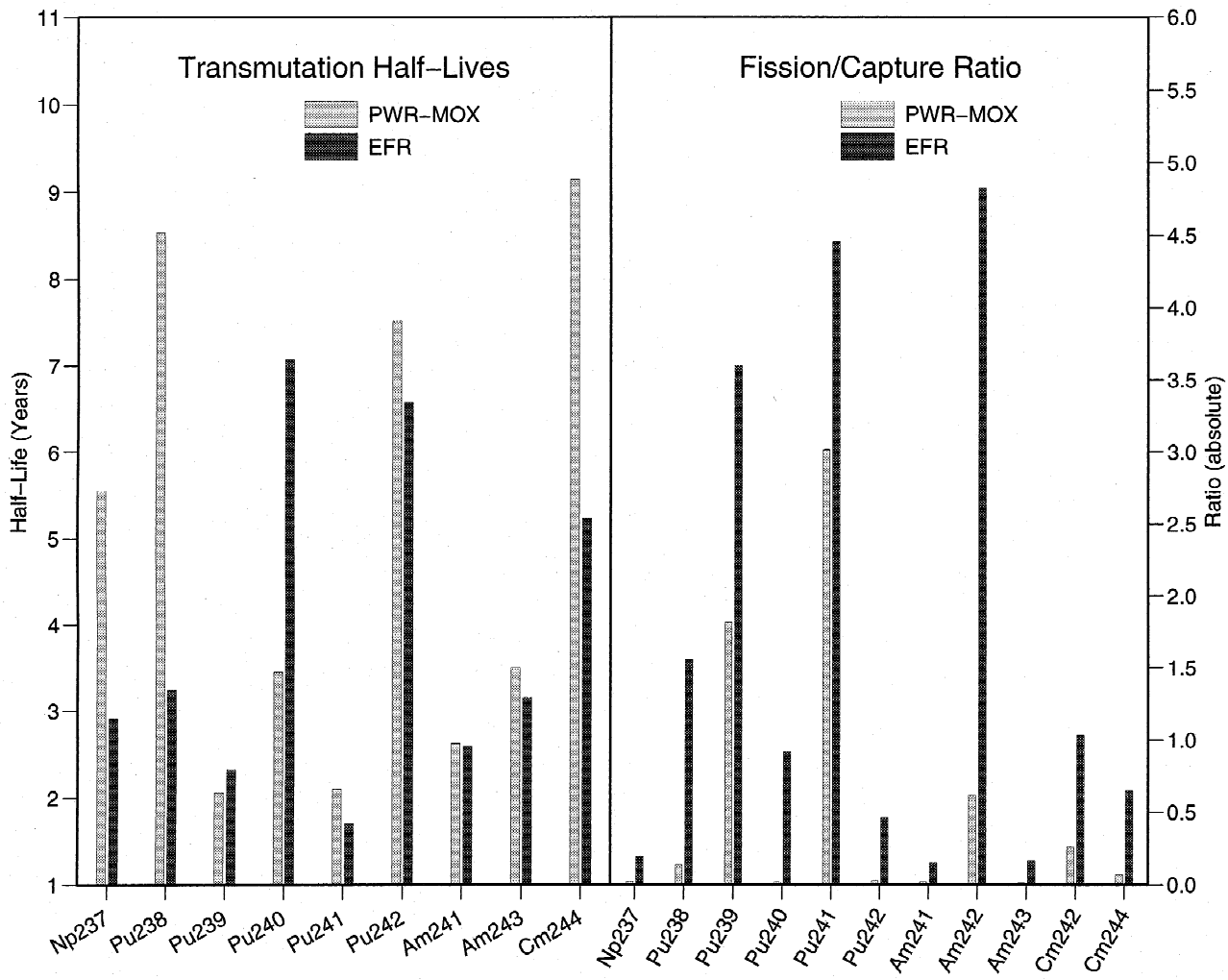

Fig. 4. Transmutation half-lives and fission/capture ratios.

fact, the coupled system of burn-up equations has to be solved. Moreover, to exhaust the abilities of actinide burner reactors, multiple recycling has to be included. To this end, in the next chapter a large step to the back-end of transmutation investigations is done by looking at calculational results for fast burner reactors coupled to PWRs in a European park of nuclear power plants.

3. Transmutation in a European Park of PWRs and fast burner reactors

The capacity of nuclear power plants in Europe, mainly PWRs, amounts to about 120 GW electric. This park of reactors may be represented by 82 UOX fuelled PWRs of the French type N4 with a nominal power of 1470 MW electric each. The production of Pu and MA is 252 kg Pu, 15 kg Np and 17 kg Am per cycle and N4. Further N4 characteristics are listed in Table 2. After an initial 30 years of sole PWR operation, the accumulated Pu amounts to 553 t at a composition of 2.6, 56.9, 26.2, 6.3, 8.0 w/o Pu238, Pu239, Pu240, Pu241, Pu242, respectively. MA are produced according to 36 t Np237, 51 t Am241, 10 t Am243.

To reduce further accumulation with continued park operation and, in particular, to make use of the energy potential of Pu, burner reactors allowing multiple recycling of Pu and MA with favourable transmutation properties were looked for. Pu can be and is already reused in thermal reactors in low-enriched (U,Pu)-MOX fuel and allows multirecycling if enriched uranium is taken for MOX fabrication [5]. However, thermal reactors have $Pu/(U+Pu)<0.1$ whereas fast reactors permit much larger fractions of Pu resulting in an increased consumption of Pu. Based upon the favourable fast reactor transmutation properties, the French CEA in 1994 suggested the (U,Pu)-MOX fuelled fast burner reactor of type CAPRA with $Pu/(U+Pu)\approx 0.45$, the latter value limited by solubility requirements during PUREX reprocessing. CAPRA characteristics are listed in Table 2. In the following, the evolution of the European park inventory is discussed with Pu and MA producing N4 PWRs being substituted by

Table 2
Characteristics of N4 PWRs and CAPRA burner reactors

	Unit	PWR N4	CAPRA
Electrical reactor power	MW	1470.0	1458.0
Thermal reactor power	MW	4000.0	3600.0
Thermal efficiency		0.367	0.405
Total heavy material	tonnes	110.4	20.98
Initial enrichment U 235	w/o	4.0	
Heavy material per reload	tonnes	22.08	6.993
Average discharge burn-up	GWd/tHM	47.5	150.8
Thermal power density	MW/tHM	36.3	171.6
Length of cycle	y	1.0	1.0
Load factor		0.717	0.802
Number of in-core/cooling/ refabrication cycles	5/5/2	5/5/2	3/3/2

CAPRA burners, the production of energy being kept constant. In Fig. 5 the flow of masses between reactors including reprocessing plants and four separate pools containing LWR Pu, burner Pu, spent U, and MA from LWR and burner operation is shown. Fission products and reprocessing losses are collected separately. To accomplish accounting of masses, besides the pool residues after park shut-down, the reactor shut-down inventories are considered. Np is recycled by homogeneous admixing to (U,Pu)-MOX fuel whereas Am is irradiated in special (U, Am)-fuel elements or pins in heterogeneous positions, favourably in outer core regions.

Refuelling of fission reactors with respect to criticality and safety needs during operation requires an adjusted amount of fresh-fuel excess reactivity which in fast reactor (U, Pu)-MOX fuel is directly related to the Pu/(U+Pu) fraction. With 'good quality' Pu taken from N4 PWRs and no admixtures of MA, reference Pu fractions in the inner and outer CAPRA core at the start-up of burner operations are 0.37 and 0.41, respectively. Homogeneous admixing of neutron absorbing Np to (U, Pu)-MOX requires replacement of U by Pu (U+Pu+Np=constant), utilization of deteriorated spent CAPRA Pu needs an additional increase in Pu.

Concerning Pu, the ultimate goal is to stop the increase of park Pu inventory. It turns out that for the CAPRA reactor with (U,Pu)-MOX fuel the upper limit of Pu/(U+Pu)≈0.45 works against quantitative recycling of burner Pu because of its quality decreasing with continued recycling. Attempts to improve 'bad quality' Pu performance by reduction of neutron leakage-diluents tentatively replaced by fuel resulted in unacceptable fuel mass increases [6]. A possibility to force down the Pu fraction in CAPRA MOX fuel is to take only part of the Pu available from CAPRA fuel reprocessing for fresh-fuel fabrication. In Fig. 6 the resulting iteratively determined fraction of recycle Pu in reload fuel, starting with 20 % and decreasing according to the decrease in Pu quality down to 15 % is shown. PWR Pu is admixed according to excess reactivity needs. Iteration is performed such that the total-Pu fraction remains on a constant level at about 45 %. In Fig. 7 the composition of CAPRA recycle Pu with decreasing quality is shown; Pu239 and Pu241 decrease, Pu238, Pu240 and Pu242 increase. The composition of the

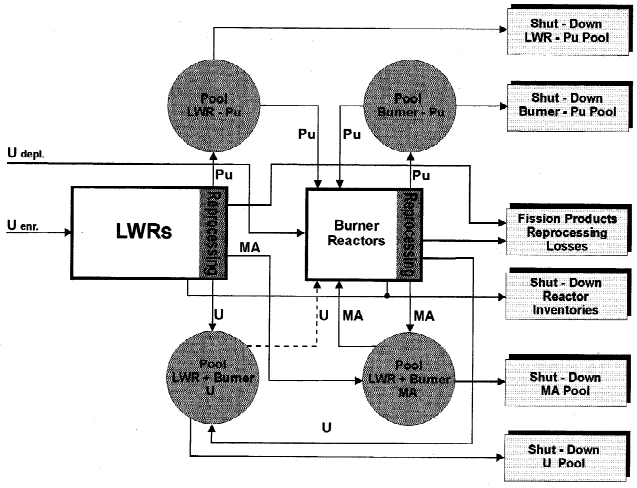

Fig. 5. Flow of masses in a park of coupled LWRs and burner reactors.

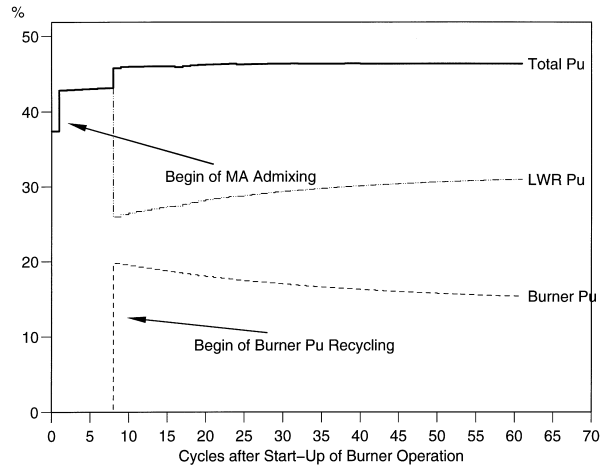

Fig. 6. Fraction of Pu in inner core CAPRA burner.

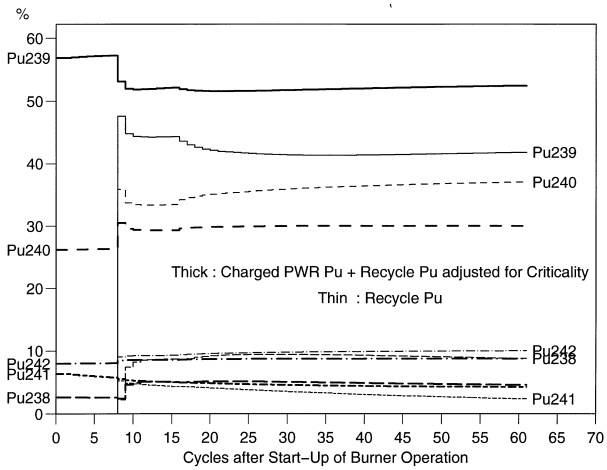

Fig. 7. Composition of CAPRA Pu.

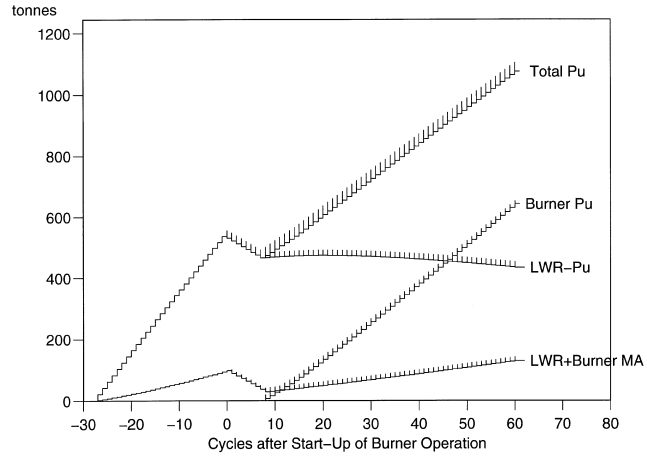

Fig. 8. Evolution of Pu and MA in 120 GW electric park.

adequately mixed reload Pu reaches equilibrium after 25 years of park operation. In Table 3 compositions of Pu in park cycle 50 after six Pu recyclings is listed. Burner Pu comprises Pu from reprocessing of irradiated (U, Am), the latter revealing an extremely large fraction of 71 % of Pu238 from Am241 (n, γ) Am242 (β^-) Cm242 (α) Pu238. The option of using Pu238 for spacelab applications etc. seems promising, separate reprocessing of spent (U,Am)-fuel, however, has to face radiation and heat production from Pu238.

To permit arbitrary continuation of park operation, the number, n_B, of CAPRA reactors substituting N4 PWRs is chosen such that in 'equilibrium' park operation with the LWR-Pu fraction in CAPRA MOX fuel, η_L, having reached 30 %, Fig. 6, the need of LWR Pu for fuelling the CAPRA burners is in balance with the amount of Pu produced by n_L N4s. With a production of LWR Pu of $p_L = 252$ kg/cycle/N4, electrical powers $E_L = 1.470$ GW, $E_B = 1.458$ GW, and a (U, Pu) charge to the burner of $c_B = 6993$ kg, see Table 2, the mass and energy balance relations, $n_L\ p_L = n_B\ \eta_L\ c_B$, $n_L\ E_L + n_B\ E_B = 120$ GW, gives an estimate of $n_B = 8.8$ CAPRA burner reactors. A larger number of burners would lead to an early exhaustion of the PWR-Pu pool with subsequent park shut-down or, for continued park operation, a return to the above PWR-Pu balanced operation after shutdown of odd burner reactors.

Table 3
Composition (w/o) of Pu in park cycle 50

Nuclide	PWR-Pu	Burner Pu	(U, Am) Pu	Reload Pu
Pu238	2.5	9.1	70.7	4.7
Pu239	57.7	41.5	9.0	52.3
Pu240	26.6	36.7	4.1	30.0
Pu241	5.1	2.7	0.02	4.3
Pu242	8.1	10.0	16.2	8.7

In Fig. 8, the evolution of Pu and MA during 30 years of sole N4 and 60 years of coupled N4-CAPRA operation is shown. Besides the parameters mentioned before, the Np admixing fraction is 5 %, (U, Am) fuel with 75 % Am added heterogeneously to the CAPRA core as an additional outer ring of the outer core, amounting to 20 % of the annual charge of heavy material, i.e. 1400 kg U + Am per CAPRA reactor per reload. Up to cycle 0, both the PWR-Pu pool and the MA pool increase from a sole operation of 82 N4 PWRs. Next, up to cycle 8, when recycle material from CAPRAs is not yet available but Pu and MA are subtracted for CAPRA fuel fabrication (MA from cycle 2), there is a strong decrease for both pools. Of course, charging this Pu to CAPRAs does not mean its burning; consideration of park shut-down inventories will account for this. Afterwards, the PWR-Pu pool stays on a rather constant level: supply and demand of PWR-Pu are approximately balanced due to the above estimation of n_B. But the pool of Pu from spent CAPRA fuel reprocessing starts being filled and only partly emptied, thus increasing with time.

First MA related investigations based on common homogeneous admixing of both Np and Am to the core fuel at a limit of 5 % from reactor safety considerations. Then neither Np nor Am were reduced sufficiently. The modified concept of heterogeneous irradiation of Am allows 5 % homogeneous admixing to the core fuel only of Np. The result, Fig. 9, is a cessation to the increase of the park Np. For heterogeneous irradiation of Am, in a first approach the neutron spectrum of the EFR radial blanket was used for determining effective neutron reaction cross-sections. A neutron flux density of 10^{15} n cm^{-2} s^{-1} was assumed. From Fig. 9 it is seen that in this approximation the net amount of park Am is increasing with time. In advanced concepts, heterogeneous irradiation of Am in moderated fuel elements is considered, e.g. by using zirconium hydride for slowing down the neutrons in blanket positions. Reactor performance will not be serious-

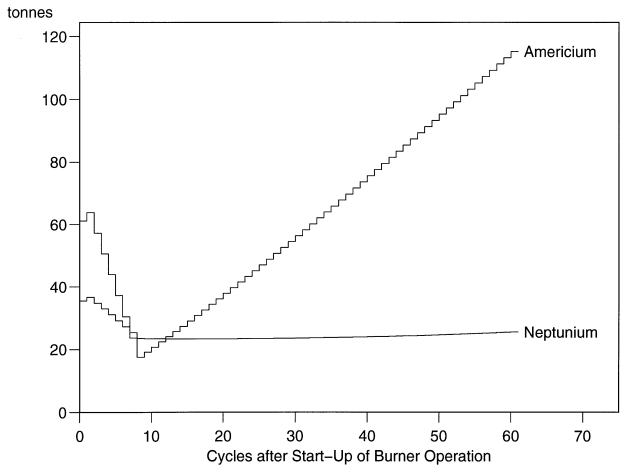

Fig. 9. Evolution of Np and Am in 120 GW electric park.

ly affected by these modifications, but Am transmutation abilities will be improved because of the spectral-shift related increase of transmutation cross-sections.

In Table 4, Pu and MA production and consumption characteristics of N4s and CAPRAs per unit of produced electrical energy are listed. The energy specific Pu and MA production rates of N4 PWRs are directly related to the cycle-specific values given at the beginning of this chapter. A Pu consumption of 65–75 kg/TWh electric is typical for CAPRAs. Using thermal efficiency and burn-up from Table 2, with the Pu fraction of 45 %, the energy specific Pu consumption of 65 kg/TWh electric can be converted to a relative Pu mass consumption $(Pu_{in}-Pu_{out})/Pu_{in}=65\times2.4\times10^{-5}\times0.405\times150/0.45=0.21$, i.e. 21 w/o of the charged Pu is burnt up to discharge. From this it is deduced that 58 % of the spent CAPRA Pu is kept in the burner Pu pool and, to reach the above stated ultimate goal, left for incineration in e.g. CAPRA-type reactors dedicated to burn even lowest-grade Pu, or in subcritical accelerator driven devices, the latter being less sensitive to deterioration of Pu. However, the CAPRA burners operating in the park turn out to be high-grade consumers of 'good and bad quality' Pu, being able to stop accumulation of 'good quality' PWR-PU and leaving behind only Pu which is deteriorated and proliferation resistant.

Heterogeneous consumption of Am is 16.4 kg/TWh. Because of the in-core production of 7.7 kg/TWh, the net consumption reduces to 8.7 kg/TWh. The Am production rates reveal a specific property of fast reactors: due to fast reactors fuelled with Pu as the source of Am, their in-core production of Am is much larger than the production of Am in UOX-fuelled PWRs, where Pu has to be built-up before being transmuted to Am.

Table 4
Production/consumption of Pu and MA in kg TWh electric

Element	Production N4	Consumption CAPRA
Pu	27.2	65.0
Np	1.63	14.1
Am	1.84	8.68[a]

[a] 7.73 homog. produced, 16.41 heterog. consumed.

The large consumption of Np of 14 kg/TWh is due to the increased amount of Np solely admixed to the core fuel. Moreover, Np incineration is enhanced by its rather low production from depleted U taken for MOX fabrication.

4. Computer codes and data

Calculations were performed with the Karlsruhe multiple-recycling scenario code KORREC using KORIGEN [7,8] as a basic module. CAPRA core neutron cross-sections were supplied by CEA [9]. Further data base on JEF [1] and on KEDAK [10].

5. Summary

In the review section, from a comparison of thermal and fast reactor neutron spectra and resulting transmutation cross-sections, fission-to-capture ratios and transmutation half-lives, the superior transmutation ability of fast reactors is recollected. Multiple recycling of Pu in fast (U, Pu)-MOX CAPRA reactors in a European 120 GW electric park with nine CAPRAs and 73 N4 PWRS, resulting in PWR-PU equilibrium, is restricted by deterioration of Pu, reactivity needs, and a Pu fraction limited by ≈45 %. The CAPRA burner turns out to be a high-grade consumer of 'good and bad quality' Pu, leaving behind Pu which is deteriorated and proliferation resistant. In equilibrium, 58 % of Pu from reprocessing of spent CAPRA fuel has to be excluded from recycling. In the park, accumulation of 1st generation PWR-Pu is stopped and can even be reduced to a low level. Further reduction of residual Pu might be achieved by means of special CAPRA-type reactors dedicated to burn even lowest-grade Pu or by accelerator-driven devices. Homogeneous 5% admixing of Np results in a constant-level Np park inventory; incineration of Np works perfectly. In an approximation, heterogeneous irradiation of Am was performed in an EFR blanket spectrum. The relatively large heterogeneous consumption is counteracted by likewise significant in-core production of Am. The result is an increase of park Am. From irradiation of Am in moderated fuel elements improved incineration is expected.

References

[1] History of JEF Evaluations, NEA Data Bank, JEF/DOC-354, 1991.
[2] A.G. Croff, M.A. Bjerke, G.W. Morrison, L.M. Petrie, Revised Uranium-Plutonium Cycle PWR and BWR Models for the ORIGEN Computer Code, ORNL/TM-6051, 1978.

[3] A. Languille, J.C. Garnier, D. Verrier, R.E. Sunderland, E. Kiefhaber, T. Newton, CAPRA Core Studies-the Oxide Reference Option, Proc. GLOBAL '95, Versailles, France, 1995, Vol. 1, p. 874.
[4] Technical Secretariat of Management Group Research and Development, MGRD (Ed.), A Review of the Collaborative Programme on the European Fast Reactor (EFR), Annual Meeting of IWGFR, IAEA, Vienna, and FRCC, CEC, Brussels, 1992.
[5] C.H.M. Broeders, Investigations Related to Build-Up of Transurania in Pressurized-Water Reactors, FZKA-5784, 1996.
[6] D. Thiem, FZK-INR (private communication, August 1997).
[7] U. Fischer, H.W. Wiese, Verbesserte konsistente Berechnung des nuklearen Inventars abgebrannter DWR-Brennstoffe auf der Basis von Zell-Abbrand-Verfahren mit KORIGEN, KFK-3014 1983 and ORNL-tr-5043.
[8] H.W. Wiese, B. Krieg, KORIGEN '95: Extension of data libraries and option for fission products from spontaneous fissions, Proceedings of the Annual Meeting on Nuclear Technology, Mannheim, Germany, 1996, p. 51.
[9] J.C. Garnier, CEA (private communication).
[10] B. Goel, B. Krieg, Status of the Nuclear Data Library KEDAK-4, KFK-3838, 1984.